CASE WESTERN RESERVE UNIVERSITY

SCHOOL OF DENTAL MEDICINE

GRADUATE STUDIES

We hereby approve the thesis of

Heather Horton

Candidate for the degree

Master of Science in Dentistry

Signed: _____
(Chairperson)

_____

_____

_____

Date: _____

A Method to Compare Relative CBCT Density in the Mandible

by

Heather Horton, D.D.S.

Submitted in partial fulfillment of the requirements for

the degree of Master of Science in Dentistry

Department of Orthodontics

Case Western Reserve University

Thesis Advisor: Mark G. Hans, D.D.S., M.S.D.

Committee Members: J. Martin Palomo, D.D.S., M.S.D.

Richard J. Jurevic, D.D.S., Ph.D.

Department of Orthodontics

School of Dental Medicine

CASE WESTERN RESERVE UNIVERSITY

DEDICATION

Rarely in life does one happen upon an individual so intrinsically kind and good that it takes your breath away. And even more rarely do you get to spend your life with that person. I dedicate this thesis to Frank, for his unrelenting love and support throughout both the formidable task of completing this thesis and my entire orthodontic residency.

ACKNOWLEDGEMENTS

Thank you to my amazing parents. Without your endless love, guidance, and tireless support, I would never be where I am today. I am extremely blessed to have you in my life.

Thank you to my siblings, Matthew and Ashley. I could not have had a better set of people to grow up with.

Thank you to Dr. Hans for your inspiration and guidance throughout this thesis process.

Thank you to Dr. Palomo for being a great program director and your help with all things imaging.

Thank you to Dr. Jurevic for your enthusiasm for dentistry and dental sciences and your gracious help on my thesis.

Thank you to the entire orthodontic faculty at Case Western Reserve University. Your selfless willingness to share your varied experiences and expertise is a very meaningful gift, one that I greatly value and will use every day of my orthodontic career.

And thank you again to Frank. Without your technical prowess this thesis and manuscript would not have any images!

A Method to Compare Relative CBCT Density in the Mandible

Abstract

by

HEATHER M. I. HORTON

Title: A Method to Compare Relative CBCT Density in the Mandible

Objective: The goal of this study was to develop a method for measuring and comparing relative densities of various regions of the mandible in growing (i.e. subadult) patients.

Materials and Methods: Density was measured on twenty-five CBCT pre-treatment images in the following four areas: head of the condyle, posterior border of the ramus near gonion, inferior border of the ramus near gonion, and near gnathion. The first three areas were normalized by dividing them by the density value found near gnathion and multiplying by 100. The density was measured in

Hounsfield Units (HU). Each measurement was repeated three times.

Results: Reliability was excellent for all measures (adjusted $R^2 \geq 0.96$). The condyle was consistently the least dense measure ranging from -181 to -1(-47 to 0 normalized to gnathion) and gnathion showed the highest density (range 329 to 647). Density values for the posterior border ranged from -56 to 229 (-17 to 35 normalized) and for the inferior border from 2 to 309 (0 to 48 normalized).

Conclusions: It is possible to measure relative density at the head of the condyle, at the posterior border of the mandible near gonion, at the inferior border of the mandible near gonion, and near gnathion in CBCT images. The normalized density measures suggest that variations in resorption and deposition patterns vary among individuals. These variations might be used by clinicians to predict mandibular growth potential for individual patients.

TABLE OF CONTENTS

DEDICATION.....2

ACKNOWLEDGEMENTS.....3

ABSTRACT.....4

LIST OF TABLES.....7

LIST OF FIGURES.....8

LITERATURE REVIEW.....9

LIT REVIEW REFERENCES.....25

STATEMENT OF THESIS.....28

MANUSCRIPT FOR PUBLICATION.....29

MANUSCRIPT REFERENCES.....58

APPENDICES

IRB Approval.....62

Further investigation—Comparing HU values to linear growth from condylion to gnathion, condylion to gonion, and gonion to gnathion.....63

Normalized values for each initial CBCT image, as well as the change (in mm) from the pre- to post- treatment images for each linear measurement.....67

LIST OF TABLES

Table 1. Averages and standard deviations for the raw Hounsfield values for all four areas measured, as well as the correlations between each of the three times the values were measured.

Table 2. Raw data—all non-normalized HU values.

Table 3. Normalized values for each pre-treatment CBCT image for the head of the condyle, posterior border of the mandible near gonion, and inferior border of the mandible near gonion.

LIST OF FIGURES

Figure 1 (a-d). Screenshots of the areas to take the circular cut for the head of the condyle (a), posterior border of the mandible near gonion (b), inferior border of the mandible near gonion (c), and near gnathion (d).

Figure 2 (a-d). Screenshots of the steps to measure the Hounsfield units for the head of the condyle.

Figure 3 (a-d). Screenshots of the steps to measure the Hounsfield units for the posterior border of the mandible near gonion.

Figure 4 (a-d). Screenshots of the steps to measure the Hounsfield units for the inferior border of the mandible near gonion.

Figure 5 (a-c). Screenshots of the steps to measure the Hounsfield units for the area near gnathion.

Figure 6 (a-c). Screenshots demonstrating how the visualization differs when changing the density and Seg bars.

LITERATURE REVIEW

Understanding growth of the craniofacial complex is an ongoing, oft-studied endeavor. Dr. Allan Brodie, 1946, described the importance of understanding facial growth more than 60 years ago, and astutely paid heed to individual variation not as abnormal, but rather as a necessity for the creation of unique individuals and therefore to be expected. Individuals are not harmonious in their variation, rather one individual can have plus and minus values for various features. Dr. Brodie believed at that time there was a good starting foundation of the knowledge of facial growth, but there was still a need for a greater understanding of where and how much growth there will be.

Specific to mandibular growth, investigators have studied the patterns, evaluated when and how fast it grows, and have developed prediction methods based dozens of different factors. Ricketts' growth prediction method employs a system of evaluating cephalometric tracing points and then adding certain amounts of growth at each

of those points (Ricketts, 1972). The amount of predicted growth at the various points is determined in relation to the other cephalometric points and constructed distances, as well by as applying other knowledge of growth and development. For example, the change in length from sella to basion should be about three fourths of the change from sella to nasion. Once this is completed for all the points, a cephalometric growth prediction tracing can be constructed. The process is rather cumbersome, therefore the process was later computerized and made commercially available.

A study in support of Rickett's analysis was completed by Kocadereli and Telli (1999). They took a sample of 40 Turkish children (20 boys, 20 girls) and took cephalometric headfilms at about age 9 and again at about age 16. The initial radiographs were used to predict, among other things, the amount of mandibular growth to occur. They found that there was fairly good correlation between the predicted and actual amount of mandibular growth and that the Rickett's analysis is a good tool to utilize when treatment planning.

Lysle Johnston, 1975, presented an alternative prediction method that was greatly simplified and utilized mean change expansion to predict mandibular growth. He created a series of grids that a practitioner could lay out over a cephalometric radiograph and then, depending on the age of the patient when the radiograph was taken, a certain amount of growth was added according to the grids, at specific points, and then the cephalometric prediction could be fully traced. Johnston made no claim that this method of prediction was exceptionally accurate, but rather that it was as accurate as any other potential prediction method available. Johnston and Greenberg, 1975, tested the Rickett's analysis against Johnston's mean change expansion grid analysis and did not find enough difference to warrant the use of Rickett's method. They found that Rickett's method was not (overall) superior to Johnston's, only finding it superior to a jejune prediction of no occurrence of growth.

Another method of mandibular growth prediction is Fishman's system of Skeletal Maturation Assessment (SMA) (Fishman, 1981). This method uses hand wrist radiographs,

evaluating six different bone areas: three on the third finger, one on the fifth finger, one on the thumb, and one in the wrist. Using those six sites there are four skeletal maturity indicators: 1. the epiphysis equaling the width of the diaphysis, 2. the appearance of the adductor sesamoid of the thumb, 3. the capping of the epiphysis, and 4. the fusion of the epiphysis. These, in combination, make 11 skeletal maturation indicators (SMI). Reaching each of these milestones indicates a certain maturational age, which is more indicative of maturation than chronologic age. In Fishman's original study on SMA, hundreds of patient's radiographs were examined, with many conclusions reached. Those conclusions related most closely to mandibular growth were that mandibular growth rate relates directly with skeletal maturation, maximum mandibular growth rate occurs later that statural height, the mandible had less total growth compared to the maxilla until the final SMA stage, where it then caught up, and the highest mandibular growth rates are found in boys. Twenty six years after Fishman's original paper on SMA, he, Turchetta and Sutelny, 2007, compared his method to both the Johnston grid analysis and the Ricketts analysis. In

the study 50 untreated subjects were used that had longitudinal lateral cephalometric headfilms and hand wrist films at ages of approximately 9, 13, and 20 years. Each method was used at age 9 years to predict age 13 and 20, and again were used at age 13 to predict age 20. Angular and linear measurements were predicted, as well as what the author called positional prediction envelopes, which were determined by making a prediction tracing using all of the angular and linear predictions and then overlaying that tracing over what actually occurred. Using paired t-tests they found that there was no significant difference between the actual and predicted values for nearly all angular and linear measurements when using the Fishman method, whereas using the Ricketts or Johnston method many less values showed a no difference between the actual and predicted (although the Johnston method was better that Ricketts). Overall the authors concluded that the Fishman SMA method was the best predictor of both short and long term growth.

Sato et al, 2001, designed a new method of mandibular growth prediction named CASMAS (computer-aided skeletal maturity assessment system) that utilized the

third middle phalanx and radius (based on Tanner et al, 1975) and automated the process using a computer algorithm. The authors' goal was to create a method that is as accurate as the TW2 method without being as technique sensitive and time consuming. The TW2 method they refer to is a method described by Tanner et al that predicts skeletal height based off of hand wrist radiographs. Twenty-two female patients formed their standards, and then a second, similar set of 22 female patients was used to test the standards. They tested it by using four different techniques that all used bone age, substituting in either the bone age calculated by the TW2 method or by their CASMAS method. The four techniques are the ossification events method, growth potential method, growth percentage method, multiple regression method, and growth chart method. The ossification events method calculates mandibular growth potential at each stage of ossification according to bone age, until the final stage of growth and adds the predicted growth potential to the present mandibular length to predict the final length. The growth potential method uses the formula growth potential = ax (bone age) + b where a=coefficient and b=constant. The growth

percentage method correlates the relative length of the mandible with bone age and uses the formula final length = [(present length)/% of final length)]*100. The multiple regression method uses the formula $y = ax_1 + bx_2 + cx_3 + d$ where y is the final length, x_1 is the present length, x_2 is the chronologic age, x_3 is the bone age, and a-d are constants determined by chronologic age group. The growth chart method, a growth curve was determined via chronologic age and bone age, and the final mandibular length was predicted from the curve. The study found that the growth potential and growth percentage methods were the best predictors, with the TW2 technique slightly edging out the CASMAS system.

The "big three" analyses—Rickett's, Johnston, and Fishman, all display some levels of success with regards to mandibular growth prediction. Inherently, however, the pattern of that mandibular growth is not mapped, as the mandible itself does not play a role in formulating the prediction. And different mandibles certainly grow different ways. Arne Bjork's hallmark research on growth patterns of the mandible show that there is great individual variation in how the mandible grows and

develops over time (Bjork, 1963). His study of mandibular growth over time was very precise, as he was able to place hundreds of metallic implants (specifically hardened tantalum) in the mandibles of growing children to study the location and magnitude of growth over time. He found that there are three general types of grower: type A—extreme vertical growers, type B—the average grower, and type C—extreme sagittal growers. Type A, or vertical growers, exhibit the following characteristics: the gonial angle decreases, resorption at the angulus, the greatest possibility for apposition under the symphysis, and the teeth tend to erupt more vertically and lingually. Type C, or sagittal growers, exhibit the following characteristics: the gonial angle increases, the greatest possibility for less resorption and even the possibility of apposition at the angulus, less likely to see apposition under the symphysis, and the teeth erupt more forwardly. Type B is the mean of all growers and this type of grower exhibits growth patterns less extreme than the other two types. Comparing an extreme vertical grower to an extreme sagittal grower certainly demonstrates the amazing variability of growth location in the mandible (which certainly could not be predicted

by observing a cervical vertebrate or hand wrist radiograph). Ideally a growth prediction method would accurately predict growth magnitude, growth location, and growth direction.

Cervical vertebral maturation as a tool to evaluate mandibular growth has been studied extensively. Baccetti, Franchi, and McNamara, 2002, most recently developed a Cervical Vertebral Maturation (CVM) method with five stages that are categorized by evaluating C2, C3, and C4. Their original CVM method included 6 stages of cervical vertebral maturations determined by evaluating five cervical vertebrae, (Franchi et al, 2000). Within those five stages, stage II indicates that the peak mandibular growth will occur within the next year, and if stage III is recorded, that peak growth has occurred within the last year. Using the CVM method, Gu and McNamara, 2007, found absolute growth occurred most between stages III and IV, with much less occurring between stages IV and V. Importantly, they also found no visible deposition occurred at the landmark pogonion, and only very little occurred inferiorly to it during adolescent growth. While this line of research is very helpful in

determining when the most growth will occur and when the peak in growth velocity will occur, it does not specifically relate to predicting the total amount of mandibular growth that is left or where that growth will occur. Chen et al, 2004, developed a technique using the CVM method to predict mandibular growth and compared it to both the growth percentage and growth potential method and found that their method was more accurate and may be a useful tool in mandibular growth prediction using a single cephalometric radiograph. This would be advantageous as it would not require an additional radiograph and exposure that using a hand wrist film does. But similarly to the Fishman method, nothing inherent to the mandible is used in this prediction method so no insight as to the specific location or pattern of mandibular growth can be assumed.

Anatomy specific to the mandible has been studied to determine its predictive capacity with relation to mandibular growth. Kolodziej et al, 2002, studied the correlation between antegonial notch depth and facial growth. They used 40 untreated patients (20 male, 20 female) from the Iowa Facial Growth Study with lateral

cephalograms taken at ages 8.5, 12, and >17 years. The antegonial notch depth was defined as the distance between the greatest point of convexity on the inferior border of the mandible to the line connecting inferior gonion to the anterior convexity point. The depth was found and then correlated to future horizontal and vertical growth. While there were a few statistically significant negative relationships between antegonial notch depth and mandibular growth, the authors deemed that none were clinically significant enough to be used in typical treatment planning.

Very little work has been done on mandibular growth in three dimensions, especially with regards to three dimensional imaging and mandibular growth. Karup et al, 2005, studied the changes that occur during mandibular growth using medical CT images taken over time on a group of patients with Apert's syndrome, especially with regards to whether or not the symphysis menti and the mandibular canals are actually stable structures to use when superimposing serial radiographs. Interestingly they found that those two structures are stable when looking strictly from a lateral view (as has been done with

lateral cephalograms in the past) but that the mandibular canals, in fact, relocate laterally as the patient grows.

Histologically, Hans and Enlow, 1995, determined there is difference in composition of bone in areas of deposition versus resorption in the mandible. Various patterns of bone deposition and resorption lead to different patterns of growth, and they separated these patterns into three general groups: type A—classic pattern, with upward and backward growth of the mandible, type B—vertical, with a decrease in the gonial angle and an increase in the vertical growth at the head of the condyle, and type C—rotational, with a forward rotation of the mandible. The varying locations of mandibular growth are crucial to remember when evaluating other methods of mandibular growth prediction that do not directly involve the mandible, as they would have no way of predicting a specific growth pattern. If there is a histological difference between areas of deposition and resorption, it is possible that there would also be a difference between areas of greater or lesser amounts of deposition, which may differ not only in histological composition, but density as well. New areas of bone are

less dense that areas of fully formed bone, as osteoid is less dense than bone at the initial stage of calcification, which is less dense than bone at the final stage of calcification (Bonucci et al, 1970). It certainly would be beneficial if there was, as histological examination of the mandible requires either a dry skull or a bone biopsy, whereas density calculation may require only an interpretation of a three dimensional radiograph.

Since the discovery of x radiation in 1895 by Wilhelm Conrad Roentgen, there has been an interest in using radiographs to measure bone density. One early technique was to incorporate a step wedge in the field of exposure to provide a reference to both assess the quality of the radiograph and to estimate bone density. The step wedge is typically made from aluminum and is small enough to fit on a radiographic film without overlapping onto the structure being imaged. The aluminum has steps which increase in thickness (and therefore radiopacity) which can be used as a guide to estimate the density of the structure being imaged (Bloxom et al, 1986). The major problem with this method was that the

density was estimated based off of the step wedge, so very slight variances in density were difficult to discern.

Another plain radiograph technique is radiographic absorpitometry, which uses a phantom that has a calibration wedge built in that can be used to estimate bone density when placed in the field of view when taking a radiograph (Cutler et al, 2005). A drawback of this method was that it is typically only useful on peripheral bones, and there is still some degree of estimation with the calibration wedge (Gulam et al, 2000).

Dual-energy X-ray Absorpitometry (DXA) is a precise method of estimating bone density, and is the gold standard for diagnosing osteoporosis (Nelson et al, 1991). A special radiographic machine, called a densitometer, uses two x-ray beams of different energy levels and determines the density of the bone based off of the absorption of those beams by the bone being irradiated. While it is very precise, it only measures areal bone density, meaning that the information if derived from a two dimensional radiograph, so it can only report information about an area, not a volume.

Quantitative Computed Tomography (QCT) has been used to determine bone density using a spiral CT and has the advantage of three dimensional, and therefore volumetric, information (Khoo et al, 2009). This method is effective and can be compared to DXA when necessary, and also has the advantage of being able to remove the soft tissues from the image before the density measurement is taken so it does not distort the values. Magnetic Resonance Imaging (MRI) has also been used to estimate bone density by using a standardized phantom made from various hydroxyapatite concentrations in water, and the measurements correlated to those found using QCT (Ho et al, 2012).

When using a spiral CT image for evaluating density, Hounsfield units are the unit of density used. The Hounsfield scale is a way of describing radiodensity (Brooks, 1977). The formula for deriving Hounsfield units is $HU = 1000 * \frac{\mu x - \mu water}{\mu water}$ where μ_x is the average linear attenuation coefficient of the substance in question and μ_{water} is the linear attenuation coefficient of water. Spiral CT images acquire information about the radiodensity of various tissues and report the density in

Hounsfield units. In spiral CT images, absolute Hounsfield unit values for various types of tissues are calculated using the above formula and are standard across machines and across images. Bates et al, 2006, found *in vitro* that the stiffness and strength of bone in the craniofacial complex both correlate to radiodensity found using a spiral CT image.

The use of spiral CT in orthodontics has been limited due to high radiation doses and lack of precise spatial resolution. In contrast, cone beam Computed Tomography (CBCT) images are gaining increasing acceptance in orthodontics as a method to capture three dimensional information about the morphology of growing patients. Because CBCT is a true three dimensional reconstruction, the image also contains information about the density of tissue. However, density values from a CBCT are not absolute and may not be able to be compared across machines or amongst different images due to different reconstruction algorithms and because the grey level are arbitrarily set and different amongst brands of CBCT machines (De Vos et al, 2009 and Mah et al, 2010).

LIT REVIEW REFERENCES

Baccetti T, Franchi L, McNamara Jr. JA. An improved version of the Cervical Vertebral Maturation (CVM) method for the assessment of mandibular growth. Angle Orthod. 2002;72(4):316-323.

Bloxom RM, Manson-Hing LR. The accuracy of an x-ray film quality-assurance step-wedge test. Oral Surg Oral Med Oral Pathol. 1986;62(4):449-458.

Bonucci E, Ascenzi A, Vittur F, Pugliarello MC, De Bernard B. Density of osteoid tissue and osteones at different degree of calcification. Calcif Tissue Res. 1970;5(2)100-107.

Brodie AG. Facial Patterns: A Theme on Variation. Angle Orthod. 1946;16:75-87.

Chen F, Terada K, Hanada K. A new method of predicting mandibular length increment on the basis of cervical vertebrae. Angle Orthod. 2004;74(5):630-634.

Cutler AM, Whitten S, Wigderowitz C. Measurement of bone mineral density from plain radiographs. J Bone Joing Surg Br. 2005;87-B:(SUPP III) 229.

Fishman LS. Radiographic Evaluation of Skeletal Maturation: A Clinically Oriented Method Based on Hand-Wrist Films. Angle Orthod. 1981;52(2):88-111.

Franchi L, Baccetti T, McNamara JA Jr. Mandibular growth as related to cervical vertebral maturation and body height. Am J of Orthod Dentofacial Orthop. 2000;118:335-340.

Gulam M, Thornton MM, Hodsman AB, Holdsworth DW. Bone mineral measurement of phalanges: comparison of

radiographic absorptiometry and area dual x-ray absorptiometry. Radiology. 2000;216:586-591.

Greenberg LZ, Johnston LE. Computerized prediction: The accuracy of a contemporary long range forecast. Am J Orthod. 1975;67(3):243-252.

Gu Y, McNamara Jr. JA. Mandibular Growth Changes and Cervical Vertebrate Maturation. Angle Orthod. 2007;77(6):947-953.

Hans MG, Enlow DH. Age-related differences in mandibular ramus growth: a histologic study. Angle Orthod. 1995;65(5):335-340.

Ho KY, Hu HH, Keyak JH, Colletti PM, Powers CM. Measuring bone mineral density with fat-water MRI: comparison with computed tomography. J Magn Reson Imaging. 2012; doi: 10.1002/jmri.23749.

Johnston LE. A simplified approach to prediction. Am J Orthod. 1975;67(3):253-7.

Khoo BCC, Brown K, Can C, Zhu K, Henzell S, Low V, Gustafsson S, Price RI, Prince RL. Comparison of QCT-derived and DXA-derived areal bone mineral density and T scores. Osteoporos Int. 2009;20:1539-1545.

Kolodziej RP, Southard TE, Southard KA, Casko JS, Jakobsen JR. Evaluation of antegonial notch depth for growth prediction. Am J Orthod Dentofacial Orthop. 2002;121:357-63.

Krarup S, Darvann TA, Larsen O, Marsh JL, Kreiborg S. Three-dimensional analysis of mandibular growth and tooth eruption. J Anat. 2005;207:669-682.

Nelson DA, Brown EB, Flynn MJ, Cody DD, Schaffer S. Comparison of dual photon and dual energy X-ray bone densitometers in a clinical setting. Skeletal Radiol. 1991;20:591-595.

Ricketts RM. A principle of arcial growth of the mandible. Angle Orthod. 1972;42(4):368-86.

Sato K, Mito T, Mitani H. An accurate method of predicting mandibular growth potential based on bone maturity. Am J Orthod Dentofacial Orthop. 2001;120:286-290.

Tanner JM, Whitehouse RH, Marshall WA, Healy MJR, Goldstein H. Assessment of Skeletal Maturity and Prediction of Adult Height: TW2 Method. Academic Press, London, 1975.

Turchetta BJ, Fishman LS, Subtelny JD. Facial growth prediction: A comparison of methodologies. Am J Orthod Dentofacial Orthop. 2007;132:439-449.

STATEMENT OF THESIS

The goal of this study is to develop a method of measuring density in the mandible on CBCT images that allows for the comparison of those values both within one image and amongst images. The areas to be measured are the head of the condyle, the posterior border of the mandible near gonion, the inferior border of the mandible near gonion, and near gnathion.

If these areas are able to be measured reliably, the density values may be able to be used to predict growth potential in patients.

A Method to Compare Relative CBCT Density in the Mandible

Authors: Heather M. I. Horton, D.D.S.[1]

J. Martin Palomo, D.D.S., M.S.D.[2]

Richard J. Jurevic, D.D.S., Ph.D.[3]

Mark G. Hans, D.D.S., M.S.D.[4]

1. Resident, Department of Orthodontics at Case School of Dental Medicine in Cleveland, OH
2. Associate Professor and Program Director, Department of Orthodontics at Case School of Dental Medicine in Cleveland, OH
3. Assistant Professor, Department of Biological Sciences at Case School of Dental Medicine in Cleveland, OH
4. Professor and Chairman, Department of Orthodontics at Case School of Dental Medicine in Cleveland, OH

Corresponding Author:

Mark G. Hans, D.D.S., M.S.D.
Case Western Reserve University
School of Dental Medicine
Department of Orthodontics
10900 Euclid Ave.
Cleveland, OH 44106

THE ANGLE ORTHODONTIST

MANUSCRIPT DRAFT

Title: A Method to Compare Relative CBCT Density in the Mandible

Objective: The goal of this study was to develop a method for measuring and comparing relative densities of various regions of the mandible in growing (i.e. subadult) patients.

Materials and Methods: Density was measured on twenty-five CBCT pre-treatment images in the following four areas: head of the condyle, posterior border of the ramus near gonion, inferior border of the ramus near gonion, and near gnathion. The first three areas were normalized by dividing them by the density value found near gnathion and multiplying by 100. The density was measured in Hounsfield Units (HU). Each measurement was repeated three times.

Results: Reliability was excellent for all measures (adjusted $R^2 \geq 0.96$). The condyle was consistently the least dense measure (range -181 to -1, -47 to 0 once normalized to gnathion) and gnathion showed the highest density (range 329 to 647). Density values for the posterior border ranged from -56 to 229 (-17 to 35 normalized) and for the inferior border from 2 to 309 (0 to 48 normalized).

Conclusions: It is possible to measure relative density at the head of the condyle, at the posterior border of the mandible near gonion, at the inferior border of the mandible near gonion, and near gnathion in CBCT images.

The normalized density measures suggest that variations in resorption and deposition patterns vary among individuals. These variations might be used by clinicians to predict mandibular growth potential for individual patients.

INTRODUCTION

Since the discovery of x radiation in 1895 by Wilhelm Conrad Roentgen[1], there has been an interest in using radiographs to measure bone density. One early technique was to incorporate a step wedge in the field of exposure to provide a reference to both assess the quality of the radiograph and to estimate bone density.[2,3,4,5] The major problem with this method was that the density was estimated based off of the step wedge, so very slight variances in density were difficult to discern. Another plain radiograph technique is radiographic absorpitometry, which uses a phantom that has a calibration wedge built in that can be used to estimate bone density when placed in the field of view when taking a radiograph.[6] A drawback of this method was that it is typically only useful on peripheral bones, and there is still some degree of estimation with the calibration wedge.[7] Dual-energy X-ray Absorpitometry (DXA) is a precise method of estimating bone density, and is the gold standard for diagnosing osteoporosis.[8,9] While it is very precise, it only measures areal bone density,

meaning that the information if derived from a two dimensional radiograph, so it can only report information about an area, not a volume. More recently, Quantitative Computed Tomography (QCT) has been used to determine bone density using a spiral CT and has the advantage of three dimensional and therefore volumetric information.[10] This method is effective and can be compared to DXA when necessary, and also has the advantage of being able to remove the soft tissues from the image before the density measurement is taken so it does not distort the values. Magnetic Resonance Imaging (MRI) has also been used to estimate bone density by using a standardized phantom made from various hydroxyapatite concentrations in water, and the measurements correlated to those found using QCT.[11]

When using a spiral CT image for evaluating density, Hounsfield units are the unit of density used. The Hounsfield scale is a way of describing radiodensity.[12] The formula for deriving Hounsfield units is HU = 1000 * $\mu x - \frac{\mu x - \mu water}{\mu water}$ where μ_x is the average linear attenuation coefficient of the substance in question and μ_{water} is the

linear attenuation coefficient of water. Spiral CT images acquire information about the radiodensity of various tissues and report the density in Hounsfield units. In spiral CT images, absolute Hounsfield unit values for various types of tissues are calculated using the above formula and are standard across machines and across images.

The use of spiral CT in orthodontics has been limited due to high radiation doses and lack of precise spatial resolution. In contrast, cone beam Computed Tomography (CBCT) images are gaining increasing acceptance in orthodontics as a method to capture three dimensional information about the morphology of growing patients. Because CBCT is a true three dimensional reconstruction, the image also contains information about the density of tissue. However, density values from a CBCT are not absolute and may not be able to be compared across machines or amongst different images due to different reconstruction algorithms and because the grey level are arbitrarily set and different amongst brands of CBCT machines.[13,14]

Enlow has mapped the areas of deposition and resorption of the human mandible using histologic

techiniques.[15] And, it is well known that areas of new bone deposition are less dense that areas of fully formed bone, as osteoid is less dense than bone at the initial stage of calcification, which is less dense than bone at the final stage of calcification.[16] Consequently, the comparison of bone densisty on a CBCT, even if they could not be converted to the same scale as spiral CT images, might be clinically useful. Therefore, the goal of this study was to develop a method for measuring and comparing relative densities of various regions of the mandible in growing (i.e. subadult) patients.

MATERIALS AND METHODS

This study was approved by the IRB Board at Case Western Reserve University. Pre- and post- treatment CBCT images were reviewed from patients previously treated at the Case Western Reserve University Graduate Orthodontic Clinic. The patient image sets were selected from all patients that have been treated in the clinic that had CBCT images taken and also met the following criteria: female, between the ages 11 years, 6 months and 12 years, 5 months at the time the CBCT image was taken, no craniofacial syndromes, and no metallic fillings or jewelry visible in the field of view on the CBCT image. From all the patients treated at the clinic, twenty-five patient images met all criteria and were included in the study. CBCT images were acquired using the Hitachi CB MercuRay using the following settings: 2mA, 120 kVp, 12 inch field of view, 512 slices, slice thickness of 0.377mm, resolution 1024x1024 pixels, 12 bits per pixel, 4096 gray scale. The Dicom files obtained from the CBCT scans were reconstructed and density measurements were made using commercially available imaging software

(Dolphin Imaging and Management Solutions, Chatsworth, California).

Hounsfield value calculations

Hounsfield values were calculated on all CBCT images. Four areas of the mandible were selected to calculate the Hounsfield values: right side head of the condyle, right side posterior border of the ramus near gonion, right side inferior border of the mandible near gonion, and near gnathion. The measurements were repeated three times for each of the sites on each image. Figure 1(a-d) shows the four areas, and figures 2(a-d), 3(a-d), 4(a-d) and 5(a-c) show the steps for isolating the Hounsfield values at each of the sites.

To calculate each measurement, the CBCT image was first turned to the right lateral view. Then the translucency bar was slid to the left to more easily visualize the borders of the sight being evaluated. Then the Seg bar was slid as far to the left as necessary to fully see the mandibular border in the area being evaluated. Figure 6 shows how sliding the bars affects the visualization of the images (sliding the translucency and seg bars does not change the calculated values, only

how they are visualized on screen[17]). The steps for calculating the values at each specific site are as follows:

Head of the condyle

Select the middle size circle cutting tool and orient the circle to a distance equal to three quarters of the diameter of the circle inferior to the most superior point on the head of the condyle (Figure 2a). The circle should also be centered antero-posteriorly in the condyle. Cut the circle, then use the inverse function so the circular slice is all that remains on the screen (Figure 2b). Rotate that remaining slice to the posterior view. Using the free-hand cutting tool, cut out and remove all structures surrounding the right side mandibular condyle section (Figure 2c). Click calculate Hounsfield value (Figure 2d).

Posterior border of the ramus near gonion

Select the middle size circle cutting tool and orient the circle so the posterior edge of the circle is touching the most convex portion of the ramus near gonion (Figure 3a). Cut the circle, then use the inverse

function so the circular slice is all that remains on the screen (Figure 3b). Rotate that remaining slice to the posterior view. Using the free-hand cutting tool, cut out and remove all structures surrounding the right side mandibular section (Figure3c). Click calculate the Hounsfield value (Figure 3d).

Inferior border of the ramus near gonion

Select the middle size circle cutting tool and orient the circle so the inferior edge of the circle is touching the most convex portion of the inferior border of the mandible near the angle of the mandible (Figure 4a). Cut the circle, then use the inverse function so the circular slice is all that remains on the screen (Figure 4b). Rotate that remaining slice to the posterior view (Figure 4c). Using the free-hand cutting tool, cut out and remove all structures surrounding the right side mandibular section. Click calculate the Hounsfield value (Figure 4d).

Near gnathion

Select the middle size circle cutting tool and orient the circle so the edge of the circle is touching

gnathion and the rest of the circle is within the borders of the mandible (Figure 5a). Cut the circle, then use the inverse function so the circular slice is all that remains on the screen (Figure 5b). Click calculate the Hounsfield value (Figure 5c).

Statistics

All Hounsfield value measurements were repeated three times. Adjusted R^2 correlations were calculated for the three trials to determine repeatability[18]. The three estimates of density were averaged for the subsequent analyses. Means and standard deviations were also calculated. ANOVA and paired t-tests were done to determine if the densities values of each site were different.

Normalization of density estimate

In an effort to improve the comparability of HU density measurements within each CBCT image, the values for the condyle as well as those for the posterior and inferior border were normalized using the density value at gnathion. This area was chosed because it is biologically stable and always had the highest density

value when compared to the other three areas in a given image.[19] The formulas used to normalize the values were $\frac{head\ of\ condyle}{gnathion} * 100$, $\frac{posterior\ border\ of\ mandible}{gnathion} * 100$, and $\frac{inferior\ border\ of\ mandible}{gnathion} * 100$.

RESULTS

The mean age was 12 years 1 month (SD 3 months). Averages, standard deviations, and reliability correlation statistics for the raw (not normalized) data are presented in Table 1. Correlations were above 96% for the head of the condyle Hounsfield values, above 99% for the posterior border of the mandible near gonion, above 99% at the inferior border of the mandible near gonion, and right at 99% for the area near gnathion. All raw, not normalized HU values for the head of the condyle, posterior border of the mandible near gonion, inferior border of the mandible near gonion, and area near gnathion are presented in table 2. The HU values for each site were statistically different from each other ($P \leq 0.0001$). Normalized values for the head of the condyle, posterior border of the mandible near gonion, and inferior border of the mandible near gonion are presented in table 3.

The head of the condyle HU values were always the least dense of the measurements, the posterior border of

the mandible the second least dense, the inferior border of the mandible near gonion the second most dense, and the area near gnathion values the most dense. The range was -181 to -1 (-47 to 0 once normalized to gnathion) for the condyle, -56 to 229 (-17 to 35 normalized) for the posterior border, 2 to 309 (0 to 48 normalized) for the inferior border, and 329 to 647 for gnathion.

DISCUSSION

Measuring the density of the mandible in the selected areas proved to be very reliable, with correlations above 0.96 across all measurements. The very high correlation coefficient across all measurements is due to the straightforward process of the measurement technique and the ease of use of the software. While the values recorded are not absolute values like those calculated from spiral CT images, they are able to be reliably measured. And by normalizing the values to the area near gnathion that has little or no remodeling during the adolescent stage of development[19], the values can be compared specifically to CBCT images that were captured using the same settings and reconstruction algorithms. Over time the algorithms used to reconstruct the 3D CBCT images may improve to more closely replicate spiral CT images and Hounsfield values[13], which will be beneficial, but as they change, new images and values derived from those images may not be able to be compared to older images and/or values previously recorded using older algorithms.

While the normalized values for the head of the condyle, posterior border of the mandible, and inferior border of the mandible always ranked from least to most dense, respectively, they were certainly not the same across each image, nor did they always relate similarly. The range of the head of the condyle normalized values was -47 to 0, the range of the posterior border of the mandible normalized values was -17 to 35, and the range of the inferior border of the mandible normalized values was 0 to 48. In addition, the range in the difference between the head of the condyle and posterior border of the mandible was 20 to 52, 33 to 65 between the head of the condyle and the inferior border of the mandible, and 6 to 25 between the inferior border of the mandible and the posterior border of the mandible. These numbers clearly show that there are a wide variety of patterns within and amongst these patients, just as there are varying patterns of growth.

There are many applications for measuring density in the craniofacial region. Beyond the increased visual information a three dimensional image provides, determining variations in density in the area of pathologic lesions may help the borders of the disease to

be more clearly identified, and the amount of tissue to be resected in more serious cases could be more accurately determined. Spiral CT images are already used as a tool for helping to identify lesions, and if CT images were able to be used in the same capacity, the amount of radiation the patient would need to be exposed to would be greatly decreased. Asymmetric growth cases could also potentially benefit from knowledge of the density in areas of abnormal growth, as it may shed light on how similar/dissimilar the pathologic site is to its corresponding structure on the opposite side. Another, novel, way to potentially use density data would be to compare the density values in areas of active deposition to the amount of future growth the patient had in that area. As mentioned earlier, Hans and Enlow determined that the histological composition of areas of deposition and resorption vary, so it is possible that those areas would also have different density values than areas that have completed growth[15]. If this is the case, it would be another way to evaluate the growth of a patient, both in terms of whether or not they have future growth remaining and, if so, the magnitude of that remaining growth.

The findings of this study are consistent with present understanding of the remodelling patterns of the mandible. The condylar head consistently showed the least dense bone and the symphysis the highest density. Density of the posterior and inferior border were more variable. It is hypothesized that newly formed bone or bone undergoing active deposition will have a lower density than bony areas undergoing resorbtion or static bony areas. Therefore, the variations shown in this study indicate that it may be possible to map the depository and resorbtive areas of the mandible to help clinicians understand the growth potential of their patients. The next steps in this line of research are to increase sample size to include male subjects, to check bilateral symmetry of these density measures (in normal and asymmetric cases), and to determine the longitudinal changes in density in these critical areas, both in this sample and others.

CONCLUSIONS

-It is possible to measure relative density at the head of the condyle, at the posterior border of the mandible near gonion, at the inferior border of the mandible near gonion, and near gnathion in CBCT images.

-The normalized density measures suggest that variations in resorption and deposition patterns vary among individuals.

-These variations might be used by clinicians to predict mandibular growth potential for individual patients.

	Mean ± Std Dev	Correlation
Head of Condyle	-99 ± 43	0.97
Posterior Border Near Gonion	77 ± 68	0.99
Inferior Border Near Gonion	143± 66	0.99
Near Gnathion	493± 97	0.99

Table 1. Averages and standard deviations for the raw Hounsfield values for all four areas measured, as well as the correlations between each of the three times the values were measured.

Pt. #	Condyle	Posterior Border	Inferior Border	Gnathion
1	-142	57	124	474
2	-95	32	157	508
3	-46	188	235	534
4	-93	50	160	617
5	-101	121	217	496
6	-38	126	222	646
7	-155	-56	2	329
8	-76	111	182	528
9	-60	109	162	459
10	-110	229	309	647
11	-47	131	174	625
12	-1	83	148	410
13	-157	-24	55	445
14	-50	78	115	446
15	-119	50	75	434
16	-51	98	153	613
17	-120	40	81	410
18	-142	77	137	489
19	-139	14	74	350
20	-108	150	191	615
21	-109	95	139	478
22	-121	76	169	461
23	-181	4	57	398
24	-132	39	117	479
25	-81	43	112	435

Table 2. Raw data—all original, not normalized HU values. The trials 1, 2, and 3 were averaged for each site.

Patient #	Head of Condyle	Posterior Border	Inferior Border
1	-30	12	26
2	-39	6	31
3	-9	35	44
4	-15	8	26
5	-20	24	44
6	-6	19	34
7	-47	-17	0
8	-14	21	34
9	-13	24	35
10	-17	35	48
11	-8	21	28
12	0	20	36
13	-35	-5	12
14	-11	18	26
15	-27	12	17
16	-8	16	25
17	-29	10	20
18	-29	16	28
19	-40	4	21
20	-18	24	31
21	-23	20	29
22	-26	16	37
23	-46	1	14
24	-28	8	24
25	-19	10	26

Table 3. Normalized values (see text for details) for each pre-treatment CBCT image for the head of the condyle, posterior border of the mandible near gonion, and inferior border of the mandible near gonion.

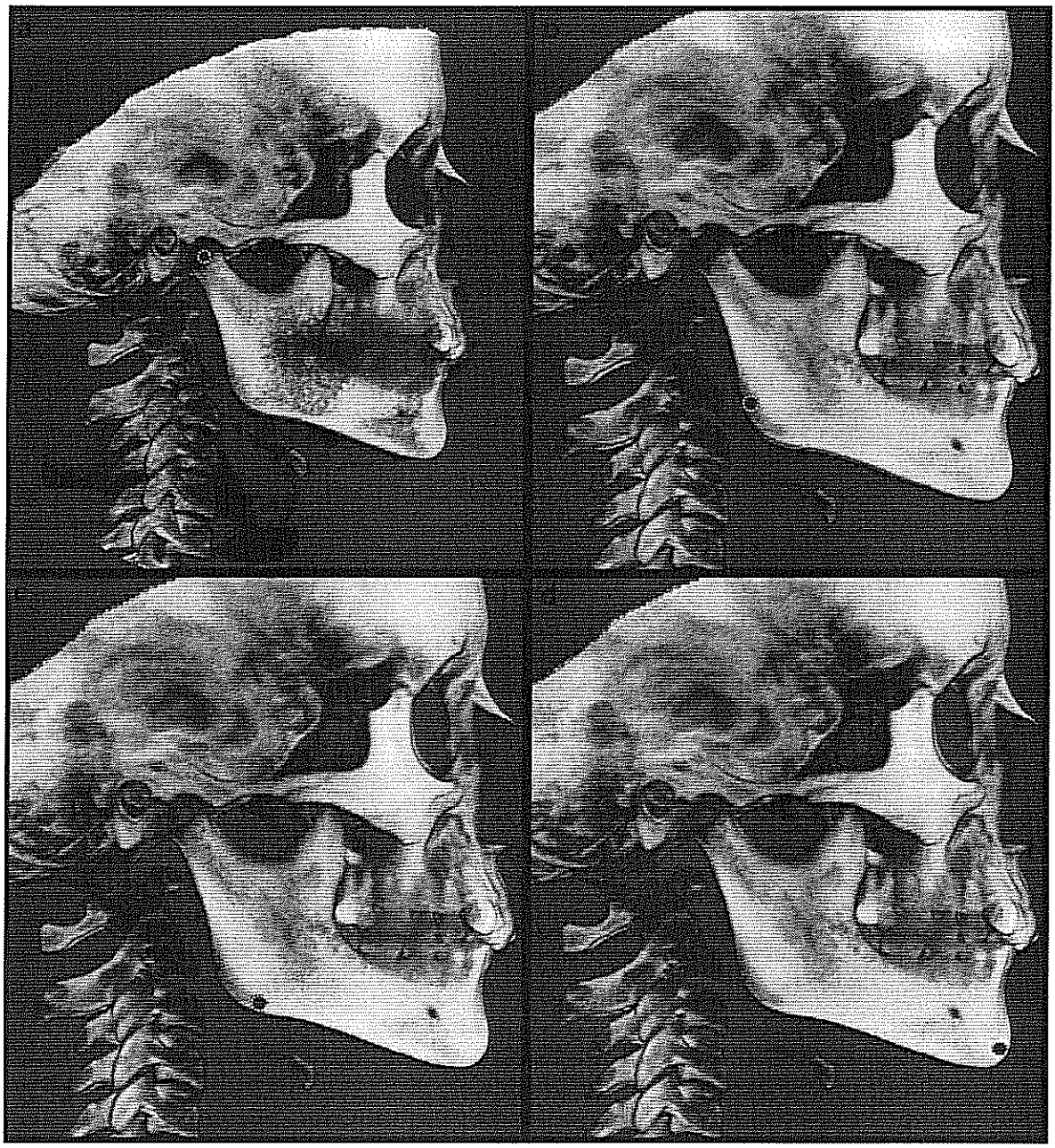


Figure 1 (a-d). Screenshots of the areas to take the circular cut (shown as a blue circle) for the head of the condyle (a), posterior border of the mandible near gonion (b), inferior border of the mandible near gonion (c), and near gnathion (d).

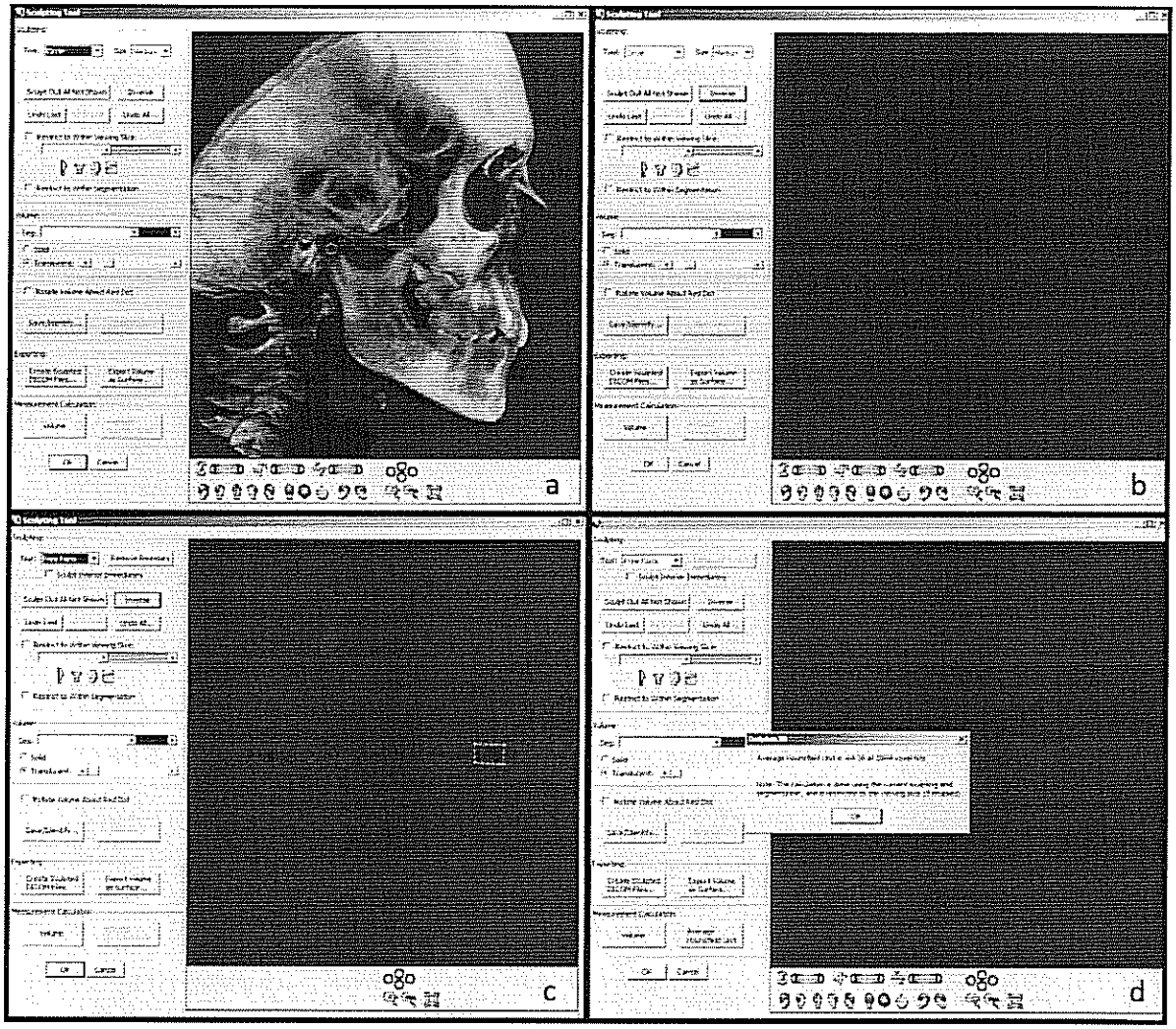


Figure 2 (a-d). Screenshots of the steps to measure the Hounsfield units for the head of the condyle.

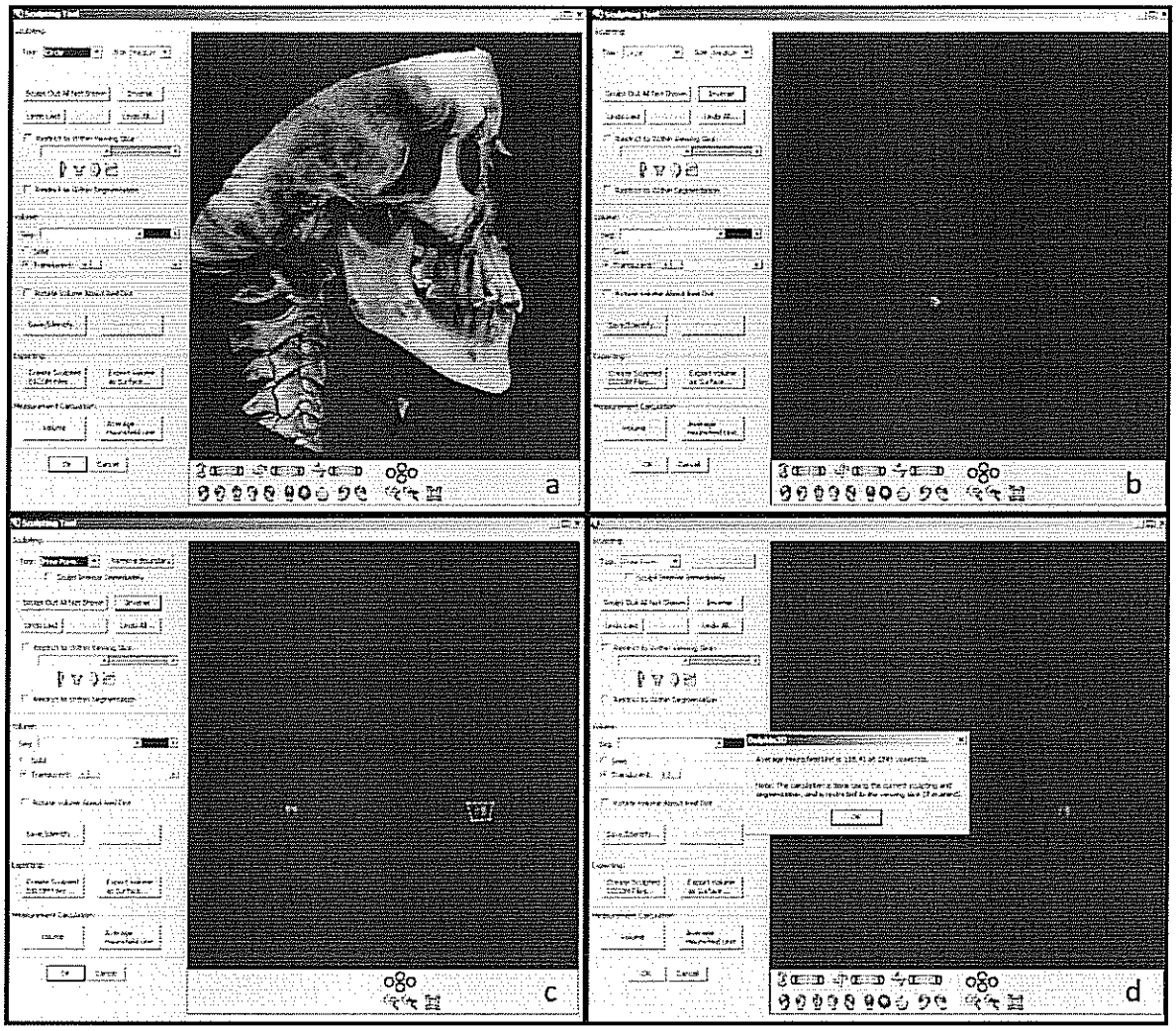


Figure 3 (a-d). Screenshots of the steps to measure the Hounsfield units for the posterior border of the mandible near gonion.

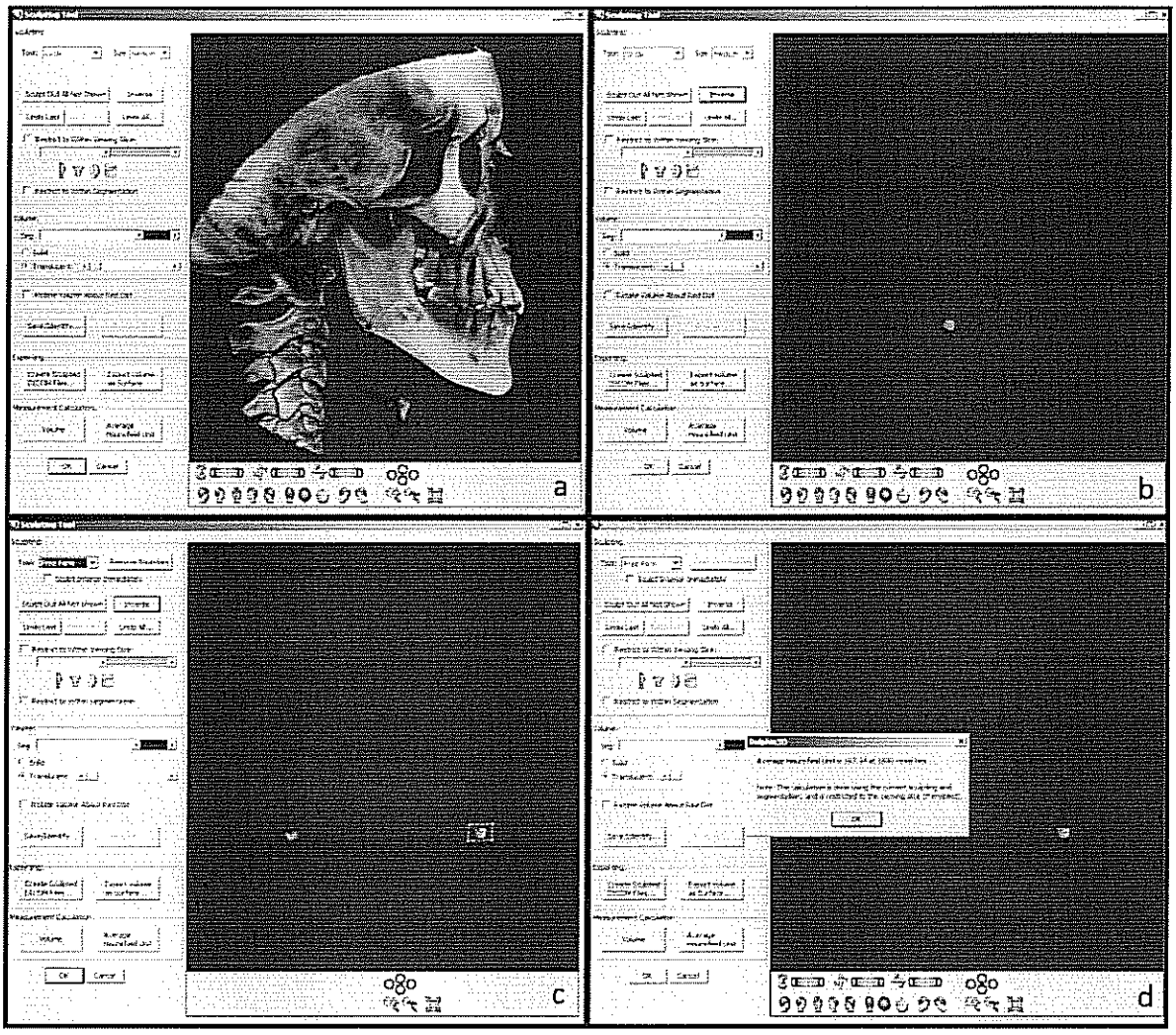


Figure 4 (a-d). Screenshots of the steps to measure the Hounsfield units for the inferior border of the mandible near gonion.

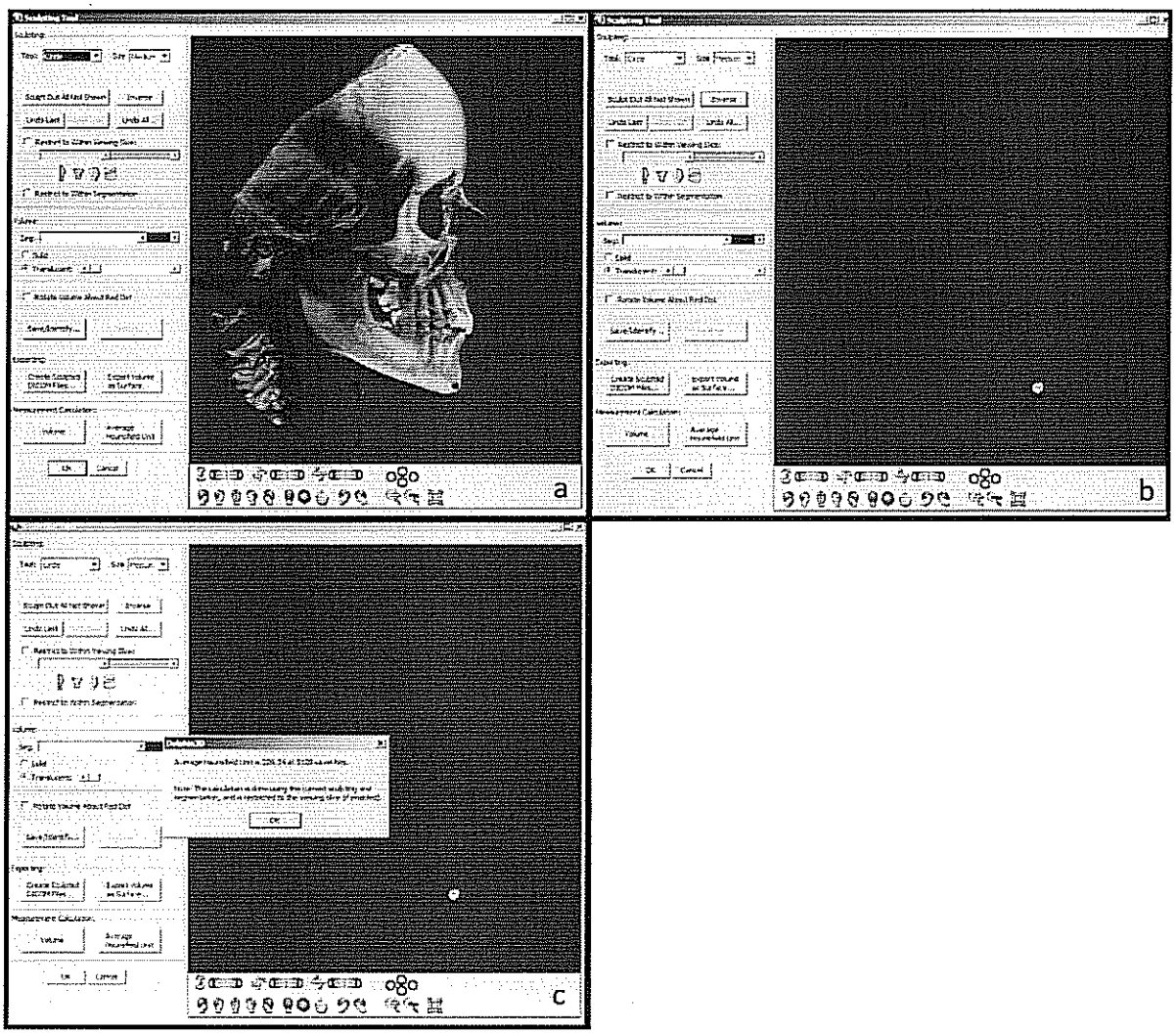


Figure 5 (a-c). Screenshots of the steps to measure the Hounsfield units for the area near gnathion.

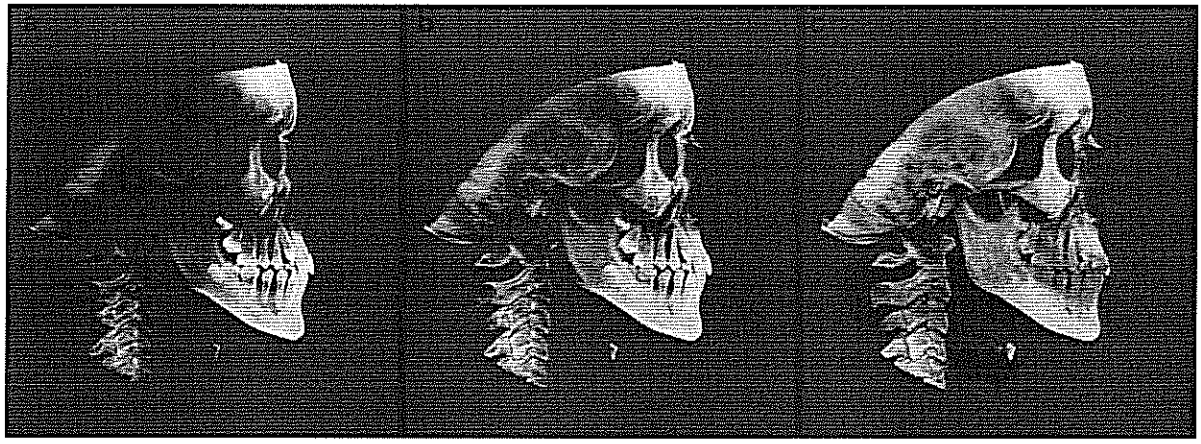


Figure 6 (a-c). Screenshots demonstrating how the visualization differs when changing the density and Seg bars.

REFERENCES

1. Discovery of x rays. Br Med J. 1945;2(4426):608-609.
2. Seemann HE, Roth B: New stepped wedges for radiography. Acta Radiol. 1960;53: 215-226.
3. Bloxom RM, Manson-Hing LR. The accuracy of an x-ray film quality-assurance step-wedge test. Oral Surg Oral Med Oral Pathol. 1986;62(4):449-458.
4. Kribbs PJ, Smith DE, Chesnut CH. Oral findings in osteoporosis. Part I: Measurement of mandibular bone density. J Prosth Dent. 1983;50(4):576-579.
5. Nackaerts O, Jacobs R, Homer K, Zhao F, Lindh C, Karayianni K, van der Stelt P, Pavitt S, Declin H. Bone density measurements in intra-oral radiographs. Oral Invest. 2007;11:225-229.
6. Cutler AM, Whitten S, Wigderowitz C. Measurement of bone mineral density from plain radiographs. J Bone Joing Surg Br. 2005;87-B:(SUPP III) 229.
7. Gulam M, Thornton MM, Hodsman AB, Holdsworth DW. Bone mineral measurement of phalanges: comparison of

radiographic absorptiometry and area dual x-ray absorptiometry. Radiology. 2000;216:586-591.

8. Nelson DA, Brown EB, Flynn MJ, Cody DD, Schaffer S. Comparison of dual photon and dual energy X-ray bone densitometers in a clinical setting. Skeletal Radiol. 1991;20:591-595.

9. Kanis JA. Gluer CC. An update on the diagnosis and assessment of osteoporosis with densitometry. Committee of Scientific Advisors, International Osteoporosis Foundation. Osteoporosis Int. 2000;192-202.

10. Khoo BCC, Brown K, Can C, Zhu K, Henzell S, Low V, Gustafsson S, Price RI, Prince RL. Comparison of QCT-derived and DXA-derived areal bone mineral density and T scores. Osteoporos Int. 2009;20:1539-1545.

11. Ho KY, Hu HH, Keyak JH, Colletti PM, Powers CM. Measuring bone mineral density with fat-water MRI: comparison with computed tomography. J Magn Reson Imaging. 2012; doi: 10.1002/jmri.23749.

12. Brooks RA. A quantitative theory of Hounsfield unit and its application to dual energy scanning. J Comput Assist Tomogr. 1977;1(4):487-493.

13. De Vos W, Casselman J, Swennen GR. Cone-beam computerized tomography (CBCT) imaging of the oral and maxillofacial region: A systematic review of the literature. Int J Oral and Maxillofacial Surg. 2009;38:609-625.

14. Mah P, Reeves TE, McDavid WD. Deriving Hounsfield units using grey levels in cone beam computed tomography. Dentomaxillofacial Radiology. 2010;39:323-335.

15. Hans MG, Enlow DH, Noachtar R. Age-related differences in mandibular ramus growth: a histologic study. 1995;65(5):335-340.

16. Bonucci E, Ascenzi A, Viittur F, Pugliarello MC, De Bernard B. Density of osteoid tissue and osteones at different degree of calcification. Calcif Tissue Res. 1970;5(2):100-107.

17. Grauer D, Cevidanes LS, Proffit WR. Working with DICOM craniofacial images. Am J Orthod Dentofacial Orthop. 2009;136:460-470.

18. Miles J. R squared, Adjusted R squared. Encyclopedia of Statistics in Behavioral Science. 2005. DOI: 10.1002/0470013192.bsa526

19. Gu Y, McNamara Jr. JA. Mandibular Growth Changes and Cervical Vertebrate Maturation. Angle Orthod. 2007;77(6):947-953.

APPENDIX 1

IRB Approval

Case Western Reserve University

CWRU Behavioral/ Social Science IRB

IRB Number: IRB-2012-129

PI: Palomo, Juan

Co-Investigator: Horton, Heather

IRB Expiration Date: 2/27/2013

Study Title: Correlation of CBCT Density Value to Mandibular Growth

Study Status: Approved - NO Recruitement

APPENDIX 2

Further investigation—Comparing HU values to linear growth from condylion to gnathion, condylion to gonion, and gonion to gnathion.

In addition to the above manuscript, additional data was collected on the given sample. It is hypothesized that the less dense an area of the mandible is (i.e. smaller Hounsfield value), the further away it is from completing growth, and therefore the larger the total increase in length will be in that area.

Linear measurements were made on both the pre- and post- treatment images, with the difference between the measurements being taken to determine the increase in length between time points. A right side only lateral cephalometric image was constructed from each Dicom file, and the points were placed and measurements taken on that image. The following points were used: condylion, gonion, and gnathion. The linear measurements calculated were from condylion to gonion, gonion to gnathion, and condylion to gnathion. The change in length (i.e. growth) data, along with the normalized HU data, is presented in

Table I. Preliminary review of the data revealed no statistical correlation between the Hounsfield values and the increases in length of the mandible, but there were some patterns worthy of examining. Large normalized measurements should have elicited very small gains in linear measurement, with very small normalized measurements correlating to large linear gains. The two patients with the largest Hounsfield values for the inferior border of the ramus both showed zero growth from condylion to gonion, but the patient with the third largest Hounsfield value at the inferior border showed 5.3mm increase in length from condylion to gonion, which was one of the largest gains. The fourth smallest Hounsfield value for the head of the condyle showed the largest gain from condylion to gnathion, and the smallest Hounsfield value in that area showed the seventh largest gain. There are more examples like these throughout the data—some promising results but many contradictions as well. This may be because while the method of calculating the density in these areas is very reliable, comparing those values to linear measurement gains may not be the most appropriate application. Bone grows appositionally

in all directions, not just in the anterior-posterior direction. A lower Hounsfield value in one of the measured areas may be more indicative of medio-lateral growth. Some values may have appeared more in line with the original hypothesis than others perhaps because in the individuals where the low values did not correlate with extensive linear growth, they may have actually been experiencing more than average gains in lateral growth in that area rather than anterior-posterior growth. Growth in other planes has historically been less studied with regards to growth, as the lateral cephalometric radiograph was one of the main tools which held no information of other dimensions. Krarup et al measured growth changes over time with CBCT images and found that there are significant changes in other planes of space other than just antero-posterior, therefore measuring volumetric changes may be more appropriate than linear[1]. In addition, it would be worthwhile to measure and evaluate the Hounsfield values in serial images to see how they change over time and how they correlate to growth. By doing so it may be found that there are certain times where density values are more or less

indicative of what will happen with regards to growth in the future.

1. Krarup S, Darvann TA, Larsen O, Marsh JL, Kreiborg S. Three-dimensional analysis of mandibular growth and tooth eruption. J Anat. 2005;207:669-682.

APPENDIX 3

Table I. Normalized values for each initial CBCT image, as well as the change (in mm) from the pre- to post-treatment images for each linear measurement.

Patient #	Head of Condyle	Posterior Border	Inferior Border	Δ Condylion to Gonion (mm)	Δ Gonion to Gnathion (mm)	Δ Condylion to Gnathion (mm)
1	-30	12	26	3.1	2.8	5.2
2	-39	6	31	8.1	2.4	8.8
3	-9	35	44	0.0	4.0	2.9
4	-15	8	26	0.2	4.2	0.9
5	-20	24	44	5.3	2.4	6.5
6	-6	19	34	3.1	6.7	8.1
7	-47	-17	0	4.5	5.5	5.8
8	-14	21	34	4.8	2.5	5.4
9	-13	24	35	1.6	1.7	2.7
10	-17	35	48	0.0	2.1	1.1
11	-8	21	28	1.6	4.7	4.0
12	0	20	36	3.3	3.7	5.3
13	-35	-5	12	2.8	3.7	5.3
14	-11	18	26	1.6	1.8	3.4
15	-27	12	17	0.6	4.0	3.4
16	-8	16	25	2.8	3.2	3.8
17	-29	10	20	0.7	3.1	4.3
18	-29	16	28	2.8	1.5	3.1
19	-40	4	21	1.2	2.4	3.3
20	-18	24	31	3.8	4.9	6.4
21	-23	20	29	4.9	4.7	7.0
22	-26	16	37	6.6	2.9	7.8
23	-46	1	14	1.1	1.1	0.4
24	-28	8	24	0.6	2.3	3.7
25	-19	10	26	2.8	3.0	4.1